microbiology
Environmental Microbiology (2016) **18**(6), 1970–1987 doi:10.1111/1462-2920.13173

Subseafloor microbial communities in hydrogen-rich vent fluids from hydrothermal systems along the Mid-Cayman Rise

Julie Reveillaud,[1†] Emily Reddington,[1] Jill McDermott,[2] Christopher Algar,[1] Julie L. Meyer,[3] Sean Sylva,[2] Jeffrey Seewald,[2] Christopher R. German[2] and Julie A. Huber[1*]
[1]*Marine Biological Laboratory, Josephine Bay Paul Center, 7 MBL Street, Woods Hole, MA 02543, USA.*
[2]*Woods Hole Oceanographic Institution, Woods Hole, MA, USA.*
[3]*Soil and Water Science Department, University of Florida, Gainesville, FL 32611, USA.*

Summary

Warm fluids emanating from hydrothermal vents can be used as windows into the rocky subseafloor habitat and its resident microbial community. Two new vent systems on the Mid-Cayman Rise each exhibits novel geologic settings and distinctively hydrogen-rich vent fluid compositions. We have determined and compared the chemistry, potential energy yielding reactions, abundance, community composition, diversity, and function of microbes in venting fluids from both sites: Piccard, the world's deepest vent site, hosted in mafic rocks; and Von Damm, an adjacent, ultramafic-influenced system. Von Damm hosted a wider diversity of lineages and metabolisms in comparison to Piccard, consistent with thermodynamic models that predict more numerous energy sources at ultramafic systems. There was little overlap in the phylotypes found at each site, although similar and dominant hydrogen-utilizing genera were present at both. Despite the differences in community structure, depth, geology, and fluid chemistry, energetic modelling and metagenomic analysis indicate near functional equivalence between Von Damm and Piccard, likely driven by the high hydrogen concentrations and elevated temperatures at both sites. Results are compared with hydrothermal sites worldwide to provide a global perspective on the distinctiveness of these newly discovered sites and the interplay among rocks, fluid composition and life in the subseafloor.

Received 11 May, 2015; accepted 1 December, 2015. *For correspondence. E-mail jhuber@mbl.edu; Tel. (+1) 508 289 7291; Fax 508-457-4727. †Present address: UMR 6197-Laboratoire de Microbiologie des Environnements Extrêmes (LM2E), Institut Universitaire Européen de la Mer (IUEM), Université de Bretagne Occidentale, Plouzané, France; CNRS, UMR6197-LM2E, IUEM, Place Nicolas Copernic, Plouzané, France; Ifremer, Centre de Brest, REM/EEP/LM2E, ZI de la Pointe du Diable, CS 10070, 29280 Plouzané, France.

Introduction

Deep-sea hydrothermal vents are energy-rich environments where phylogenetically and physiologically diverse microbial communities thrive both above and below the seafloor. Microbial communities are especially enriched in regimes where oxygenated seawater mixes with reduced hydrothermal fluids, thus providing abundant sources of oxidants and reductants for microbial metabolism in a thermal regime that can support life (Kelley *et al.*, 2002). These mixed fluids, termed diffuse vents, offer a window into microbial communities beneath the seafloor (Huber and Holden, 2008), and have previously been found to host diverse bacterial and archaeal populations (Takai and Horikoshi, 2000; Huber *et al.*, 2007; Perner *et al.*, 2007; Nunoura and Takai, 2009; Akerman *et al.*, 2013; Anderson *et al.*, 2013). The population structure and functional repertoire of these microbial communities are intimately linked to the physical and chemical environment, both of which, in turn, are directly influenced by the geologic setting.

Most previous microbial characterizations of subseafloor communities have focused on mafic (basalt)-hosted systems. The discoveries of diverse ultramafic (peridotite)-influenced hydrothermal systems, as well as back-arc and other types of deep-sea volcanism, have expanded the known range of geologic, physical and geochemical conditions that support microbial life (Takai *et al.*, 2004; 2008; Kelley *et al.*, 2005; Brazelton *et al.*, 2006; Perner *et al.*, 2007; 2010; Nunoura and Takai, 2009; Huber *et al.*, 2010; Takai and Nakamura, 2010). Microbial characterization of the few known ultramafic sites shows that microbial assemblages are compositionally and functionally distinct when compared with nearby and distant mafic-hosted counterparts (Schrenk *et al.*, 2004; Kelley *et al.*, 2005; Nercessian *et al.*, 2005; Brazelton *et al.*, 2006; 2011; 2012; Perner *et al.*, 2007; 2010; Flores *et al.*, 2011; Roussel *et al.*, 2011). Commonly detected organisms in

these ultramafic sites include abundant methane- and hydrogen-metabolizing chemolithoautotrophs, which are often present in relatively lower abundance in mafic-hosted systems (Flores *et al*., 2011; Ver Eecke *et al*., 2012). It is believed that the difference in microbial population structure and function between mafic and ultramafic sites reflects the high concentrations of dissolved hydrogen and carbon in hydrothermal fluids at ultramafic-hosted systems (McCollom and Shock, 1997; Takai *et al*., 2004; McCollom, 2007; Amend *et al*., 2011; Ver Eecke *et al*., 2012). Hydrogen is particularly important because it can be used to reduce ferric iron, sulfur species, oxygen and nitrate, for example, and hydrogen-driven microbial ecosystems have been described both in terrestrial habitats (Stevens *et al*., 1995; Chapelle *et al*., 2002; Brazelton *et al*., 2013) and the marine environment at deep-sea hydrothermal vents (Takai *et al*., 2004; 2006; Kelley *et al*., 2005; Nealson *et al*., 2005; Brazelton *et al*., 2012; Ver Eecke *et al*., 2012; Schrenk *et al*., 2013). Thermodynamic studies of hydrothermal fluids at both mafic and ultramafic sites also suggest a critical role for hydrogen and methane in structuring microbial communities at deep-sea hydrothermal vents. In particular, thermodynamic models predict that ultramafic-hosted systems are capable of providing almost twice as much energy as mafic-hosted systems due to enrichment of fluids in hydrogen and methane (McCollom, 2007; Takai and Nakamura, 2010; Amend *et al*., 2011).

Located on Earth's deepest and slowest spreading mid-ocean ridge, the study site is situated in the western Caribbean, where the axial rift valley floor occurs at a depth of ~ 4200–6500 m (Fig. S1; Kinsey and German, 2013). In 2009–2010, two novel hydrogen-rich vent sites were discovered along the Mid-Cayman Rise (MCR): *Piccard*, the world's deepest hydrothermal vent field, which is basalt-hosted and situated at a depth of 4960 m; and *Von Damm*, an ultramafic-influenced system that is located at a lateral distance of just ~ 20 km from *Piccard*, but at a much shallower depth of 2350 m, near the summit of an oceanic core complex (German *et al*., 2010; Connelly *et al*., 2012; Kinsey and German, 2013). The Piccard hydrothermal field is hosted in a classically neovolcanic setting atop a volcanic spur, which comprised exclusively mounded pillow basalts. There is no geologic evidence for ultramafic rocks in the vicinity of the Piccard hydrothermal field, nor in any other comparable neovolcanic ridge-axis settings, worldwide (Beaulieu *et al*., 2013; Kinsey and German, 2013). What is novel about the Piccard hydrothermal field, compared with all other neovolcanically hosted hydrothermal fields, is its extreme depth: at 4960 m, it is more than 800 m deeper (hence, at higher pressure) than all previously reported mid-ocean ridge hydrothermal fields (Beaulieu *et al*., 2013). The end-member vent fluids at Piccard are acidic (pH 3.2) with high sulfide (12.3 mM) and hydrogen (20.7 mM), but very little methane is present (0.13 mM), which is consistent with a basalt-dominated site (McDermott, 2014; Reeves *et al*., 2014). In contrast, the Von Damm site, located at 2350 m on an oceanic core complex, is thought to be influenced by reactions with ultramafic rocks (German *et al*., 2010; Connelly *et al*., 2012). No basalt has been found at this site (Connelly *et al*., 2012; Bennett *et al*., 2013); end-member fluids show chemical compositions that are only slightly acidic (pH 5.6), with up to 19.2 mM hydrogen and 2.8 mM methane, consistent with the presence of ultramafic host rocks (Reeves *et al*., 2014; McDermott *et al*., 2015). Here, we report on the first microbiological characterization of the subseafloor microbial communities in fluids venting at each site using a combination of chemical measurements, energetic modelling, total cell and domain-specific enumeration, targeted stable isotope tracing experiments, and 16S rRNA gene amplicon and metagenomic sequencing. With these data, we compare the potential energy available for microbial metabolism and the subseafloor microbial community diversity, function and activity at the two newly discovered vent fields to hydrothermal sites worldwide to provide new insights into subseafloor microbial communities at deep-sea hydrothermal vents.

Results

Diffuse fluids sampled for this study ranged in temperature from 18 to 119°C and were characterized by hydrogen sulfide concentrations that varied from below detection (< 0.2 mM) to 2.4 mM (Table 1). The pH (25°C) of the sampled diffuse vents varied from 5.9 to 7.1 at Piccard and from 6.3 to 7.8 at Von Damm (Table 1). At both sites, the magnesium concentration (52.5 mM in seawater and ~ 0 in end-member hydrothermal vent fluids) of the mixed fluids indicate that they contained 27–99% seawater (Table 1). The maximum temperature measured during fluid sampling is reported, but in many cases large fluctuations in temperature were observed during fluid collection, which often took up to 30–40 min per sample. Methane, carbon dioxide and hydrogen were not measured in the mixed fluids sampled with the Mat sampler because the device is not gas-tight. End-member concentrations of volatiles are from Reeves and colleagues (2014) and McDermott and colleagues (2015), and represent samples collected with isobaric gas-tight samplers (Seewald *et al*., 2001). At Von Damm, no microbial mats were visible, but at Piccard white filamentous bacteria coated weathered sulfides ('Fuzzy Rocks', Fig. S2). These microbial mats were not associated with venting fluids.

Total microbial cell counts in the fluids ranged from 3×10^4 to 3×10^5 cells ml^{-1}, with background seawater concentrations of $1–2 \times 10^4$ cells ml^{-1} (Table 2). Distinct cell morphologies and clusters of cells not visible in back-

Table 1. Physical and chemical characteristics of the samples analysed in this study.

Vent site: Vent field	Tmax (°C)	pH	H_2S (mM)	Mg (mM)	SiO_2 (mM)	H_2 (mM)	CH_4 (mM)	ΣCO_2 (mm)
End-Member, Beebe #3, Piccard, BVM	397	3.2	12	0	–	20.7	0.123	25.7
Shrimp Gulley #1: Piccard, BSM	24	6.7	0.3	51.6	< 0.6			
Shrimp Gulley #2: Piccard, BSM	108	6.7	0.2	50.9	0.64			
Hot Chimlet: Piccard, BVM	106	7	< 0.2	52.2	< 0.6			
Shrimp Canyon: Piccard, BVM	44	6.4	0.2	49.1	0.67			
Base of Lung Snack: Piccard, BWM	38	6.7	0.3	52.5	< 0.6			
X-19 at BV #4: Piccard, BVM	18	6.8	0.2	51.2	< 0.6			
Shrimp Vegas: Piccard, BVM	29	7.1	0.4	52.1	< 0.6			
Fuzzy Rocks 1, 2: Piccard, BVM	–	–	–	–	–			
End-Member, Von Damm	226	5.6	3.2	0	–	19.2	2.84	2.78
Old Man Tree: Von Damm	114	6.9	2.44	14	5.33			
Ravelin #1: Von Damm	87	7.4	0.2	49.6	< 0.6			
Ravelin #2: Von Damm	86	6.3	0.9	15.8	4.23			
Hot Cracks #1: Von Damm	119	7.8	0.3	48.4	0.65			
Hot Cracks #2: Von Damm	26	7.7	0.3	51.6	< 0.6			
Shrimp Hole: Von Damm	50	7.5	0.5	47.1	< 0.6			
White Castle: Von Damm	91	7.4	0.3	49.5	< 0.6			
Ginger Castle: Von Damm	47	6.7	0.3	37.3	2.35			
Main Orifice: Von Damm	109	7.1	0.2	47.4	0.72			
Seawater: Off Axis Von Damm	5	8.1	0	52.4	0.1			
Seawater: Off Axis Piccard	5	8.1	0	52.5	0.1			

End-Member data from Reeves and colleagues (2014) and McDermott and colleagues (2015).
BSM, Beebe Sea Mound; BVM, Beebe Vents Mound; BWM, Beebe Woods Mound.; mM, mmol l^{-1}; mm, mmol kg^{-1}.

ground seawater were seen, including large filaments and mineral surfaces colonized by microbial cells (Fig. S3; Breier *et al*., 2012). These results indicate local enrichment of microbial communities in the venting fluids, distinct from background seawater populations, and are consistent with previous enumerations of microbial cells in venting fluids (e.g. Huber *et al*., 2002). In the two samples with the lowest magnesium concentrations at Von Damm (Old Man Tree and Ravelin #2; Table 1), and thus the highest fraction of end-member hydrothermal fluid, cells were not countable via microscopy due to mineral precipitation (Table 2). Quantitative PCR of these two fluid samples indicate they had the lowest gene copy numbers among all samples (Table 2). Overall, the quantitative PCR data showed wide ranges in 16S rRNA gene copy numbers, from less than 5000 gene copies per nanogram

Table 2. Microbiological characteristics of the samples used in this study.

Vent site: Vent field	Cells ml^{-1}	Average bacterial 16S rRNA gene copies per ng extracted DNA (±std dev)	Average archaeal 16S rRNA gene copies per ng extracted DNA (±std dev)	Methanogenesis via formate
Shrimp Gulley #1: Piccard, BSM	1.27×10^5	8.7×10^5 ($\pm 1.8 \times 10^5$)	2.0×10^4 ($\pm 7.5 \times 10^1$)	No
Shrimp Gulley #2: Piccard, BSM	1.4×10^5	9.6×10^6 ($\pm 4.1 \times 10^6$)	3.8×10^3 ($\pm 1.2 \times 10^2$)	No data
Hot Chimlet: Piccard, BVM	5.45×10^4	1.1×10^7 ($\pm 2.5 \times 10^6$)	8.0×10^5 ($\pm 8.1 \times 10^4$)	No
Shrimp Canyon: Piccard, BVM	5.2×10^4	1.2×10^6 ($\pm 2.0 \times 10^5$)	2.1×10^4 ($\pm 3.6 \times 10^3$)	No
Base of Lung Snack: Piccard, BWM	1.37×10^5	6.6×10^5 ($\pm 1.1 \times 10^5$)	1.3×10^5 ($\pm 4.1 \times 10^4$)	No data
X-19 at BV #4: Piccard, BVM	7.27×10^4	4.5×10^6 ($\pm 1.0 \times 10^6$)	1.2×10^4 ($\pm 1.9 \times 10^3$)	No data
Shrimp Vegas: Piccard, BVM	1.64×10^5	2.4×10^7 ($\pm 5.5 \times 10^6$)	1.5×10^4 ($\pm 7.7 \times 10^2$)	No data
Fuzzy Rocks 1, 2: Piccard, BVM	no data	2.5×10^6 ($\pm 3.1 \times 10^5$)	5.1×10^3 ($\pm 1.2 \times 10^2$)	No data
Old Man Tree: Von Damm	NC	1.7×10^5 ($\pm 2.6 \times 10^4$)	3.3×10^3 ($\pm 5.9 \times 10^2$)	No
Ravelin #1: Von Damm	7.05×10^4	1.0×10^6 ($\pm 1.1 \times 10^5$)	8.3×10^4 ($\pm 4.4 \times 10^3$)	No
Ravelin #2: Von Damm	NC	2.3×10^4 ($\pm 2.9 \times 10^3$)	5.0×10^3 ($\pm 4.7 \times 10^2$)	No
Hot Cracks #1: Von Damm	2.47×10^5	2.6×10^6 ($\pm 1.1 \times 10^6$)	8.5×10^3 ($\pm 2.3 \times 10^3$)	No
Hot Cracks #2: Von Damm	9.80×10^4	5.9×10^5 ($\pm 1.7 \times 10^5$)	1.3×10^4 ($\pm 7.1 \times 10^2$)	No
Shrimp Hole: Von Damm	2.69×10^5	4.9×10^6 ($\pm 1.4 \times 10^6$)	9.5×10^4 ($\pm 1.4 \times 10^4$)	No
White Castle: Von Damm	2.75×10^5	4.8×10^5 ($\pm 1.4 \times 10^5$)	3.9×10^4 ($\pm 6.0 \times 10^2$)	No data
Ginger Castle: Von Damm	1.08×10^5	1.1×10^6 ($\pm 1.3 \times 10^5$)	1.1×10^5 ($\pm 1.7 \times 10^4$)	Yes
Main Orifice: Von Damm	2.97×10^4	3.7×10^5 ($\pm 5.6 \times 10^4$)	1.4×10^5 ($\pm 2.3 \times 10^4$)	Yes
Seawater: Off Axis Von Damm	1.84×10^4	4.9×10^5 ($\pm 1.10 \times 10^5$)	1.7×10^5 ($\pm 1.6 \times 10^4$)	No data
Seawater: Off Axis Piccard	1.15×10^4	no data	No data	No data

NC, Cells were not countable due to mineral precipitation.
BSM, Beebe Sea Mound; BVM, Beebe Vents Mound; BWM, Beebe Woods Mound.

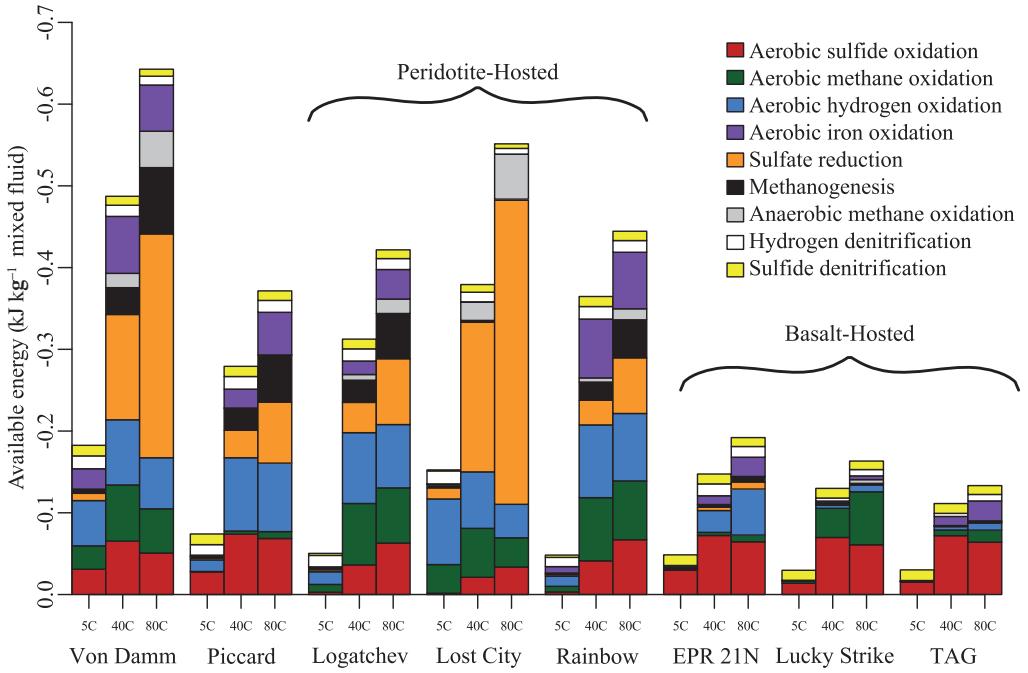

Fig. 1. Catabolic energies (in kJ kg^{-1} mixed vent fluid) available from key redox reactions in eight hydrothermal systems hosted in peridotite and basalt at three different temperatures: 5°C, 40°C and 80°C.

extracted DNA to close to 1×10^7 gene copies per nanogram extracted DNA (Table 2). Assuming the total microbial community is represented by a sum of the bacterial and archaeal gene copies, qPCR results indicate that bacteria comprise 72% to nearly 100% of the microbial populations in the vent fluids, while archaea represent < 1% to almost 28% in the same samples.

Targeted stable isotope tracing experiments were carried out to detect biological utilization of formate and dissolved inorganic carbon in the generation of methane at 70°C under anaerobic conditions. At Von Damm, stable isotope tracing experiments indicate methanogenesis with formate as a substrate is occurring at 70°C at two sites, Ginger Castle and the Main Orifice (Table 2). No methanogenic activity was detected in any tested Piccard vent fluids with either substrate (Table 2).

Thermodynamic modelling

To evaluate the potential energy available for microbial metabolism at the Piccard and Von Damm vent fields, equilibrium thermodynamic reaction-path modelling of seawater mixing with end-member hydrothermal vent fluid was carried out, and the available energy from key redox reactions shown in the *Supporting information* was calculated at 250 bar and three different temperatures: 5°C, 40°C and 80°C (Fig. 1). Results are compared with those from other peridotite-hosted and basalt-hosted vent fields previously reported by Amend and colleagues (2011). In all cases, the available energy increases with increasing temperature, and at each temperature the Von Damm vent fluids have the highest catabolic energy available compared with all other sites (Fig. 1). The catabolic energies available for key redox reactions are very similar between Von Damm and Piccard, with the major differences being more energy available overall at Von Damm, and in particular more energy yields from both aerobic and anaerobic methane oxidation at this site (Fig. 1). Similar energy profiles are seen at the peridotite-hosted Lost City, Logatchev and Rainbow sites, although the energy yields from iron oxidation and methanogenesis at Lost City are negligible (Fig. 1). The basalt-hosted EPR, Lucky Strike and TAG sites yield both lower available energies overall, and an almost complete absence of available energy for sulfate reduction, methanogenesis and anaerobic methane oxidation (Fig. 1). Instead, the energy availability at these systems is dominated by aerobic processes, particularly sulfide oxidation, but also methane oxidation, iron oxidation and aerobic hydrogen oxidation, depending on the concentrations of the particular electron donors in the end-member hydrothermal fluid. At low temperatures, aerobic reactions dominate peridotite-hosted systems, although lower sulfide concentrations place less emphasis on sulfide oxidation. As temperatures increase, high H_2 and CH_4 concentrations promote a shift from aerobic metabolism to anaerobic

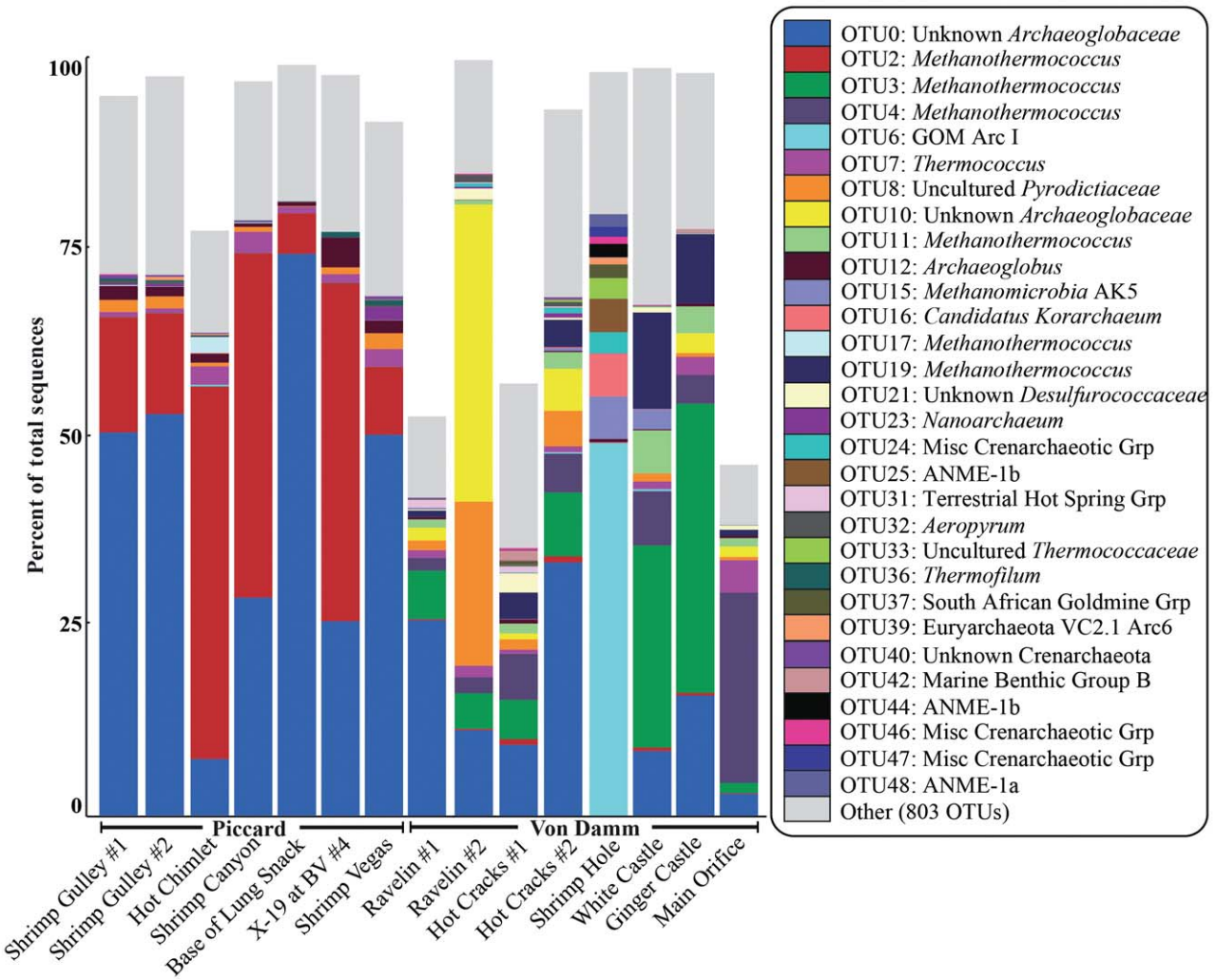

Fig. 2. Relative abundance of dominant archaeal 96% OTUs and their taxonomic assignment for rock and vent fluid samples from Piccard and Von Damm. The 30 most dominant OTUs are shown, while the others are collapsed into 'Other'.

hydrogenotrophic metabolisms (methanogenesis and sulfate reduction), and to a lesser extent anaerobic methane oxidation.

Phylogenetic diversity of microbial communities

All samples were successfully amplified using bacterial and archaeal primers, with the exceptions of Old Man Tree and 5000 m seawater. In total, 7 144 759 bacterial and 5 009 799 archaeal high-quality reads spanning the hypervariable region V6 of the 16S rRNA gene were obtained from Von Damm and Piccard vent fluids. Clustering analysis of all sequences at 96% similarity resulted in 15 981 bacterial and 961 archaeal OTUs. Vent fluid microbial communities showed a membership that was distinct from those in the non-hydrothermal background seawater at both sites, as well as from the Fuzzy Rocks (Fig. S4). In all subsequent analyses, only vent-specific OTUs (14 174 bacterial and 833 archaeal) were considered to allow for closer examination of vent-specific microbial populations.

Archaeal diversity

The most frequently recovered archaeal V6 sequences detected at both vent fields belonged to the anaerobic hyperthermophilic *Archaeoglobaceae*, with one lineage (OTU0) representing up to 74% and 33% of the archaeal sequences at Piccard and Von Damm respectively (Fig. 2). Another *Archaeoglobacae* OTU (OTU10) was highly abundant at Von Damm (up to 39% in some sites), but was present at very low relative abundance (maximum 0.002%) at Piccard. The majority of *Archaeoglobaceae* could not be resolved to the genus level using the V6 region of the 16S

rRNA gene, although up to 4% of the sequences were assigned to the genus *Archaeoglobus* at Piccard (OTU12). To obtain more phylogenetic resolution, full-length 16S rRNA archaeal genes were amplified, cloned and sequenced from Hot Cracks #2 (Von Damm) and Base of Lung Snack (Piccard). The most abundant clone sequence recovered was 100% identical in the V6 region to archaeal OTU0, the most abundant archaeal sequence obtained with the Illumina sequencing. Across the entire 16S rRNA gene, the clone sequences were ~ 96% similar to both *Ferroglobus placidus* and *Archaeaoglobus profundus*, although phylogenetic reconstruction indicated they are more closely related to the *Archaeoglobus* than Ferroglobus (Fig. S5). An additional three *Archaeoglobus* clones were recovered from Von Damm and were 93% similar to *Archaeoglobus sulfaticallidus*.

Thermophilic methanogenic archaea belonging to the genera *Methanothermococcus* were detected at all vent sites with 16S rRNA tag sequencing, although each site was dominated by different OTUs within this genus (Fig. 2). *Methanothermococcus* OTU2 represented up to 49% of the sequences at Piccard while it represented only 0.8% of the sequences at Von Damm. At the latter site, three distinct lineages of *Methanothermococcus* were found, representing more than 38% (OTU3), 25% (OTU4) and 13% (OTU19) of all archaeal sequences respectively. These OTUs were rarely observed (< 0.07%) at Piccard. Finally, OTU11 and OTU17 within the *Methanothermococcus* were found exclusively at Von Damm and Piccard respectively (Fig. 2).

Many other sequences related to both cultivated, high-temperature, anaerobic archaea and uncultivated archaeal lineages were detected in the venting fluids. *Thermococcus*, a group of high temperature heterotrophic anaerobes that were successfully cultivated from Piccard (Breier *et al*., 2012), represented up to 4% of the sequences (OTU7) at Von Damm and 3% at Piccard (Fig. 2). The GOM Arc I clade within the *Methanosarcinales*, a group previously described from Gulf of Mexico methane seeps and mud volcanoes, represented up to 49% of the sequences (OTU6) at the Shrimp Hole vent at Von Damm. It was a minor component of all other samples at both sites (Fig. 2). Another group of *Methanomicrobia* (Class AK5, OTU15) was also abundant at Shrimp Hole. The anaerobic methane-oxidizing archaea (ANME) group ANME-1b was enriched at Shrimp Hole and was also detected at a number of other sites at Von Damm, but at less than 0.004% at Piccard. ANME-1a (OTU48) was only found at Shrimp Hole. Sequences identified as South African Gold Mine (SAGMEG, OTU37), the Miscellaneous Crenarchaeotic Group (MCG, OTU24), Terrestrial Hot Spring Thaumarchaeota (THSCG, OTU31), and Marine Benthic Group B (OTU42) were also detected almost exclusively at Von Damm vent sites (Fig. 2).

Bacterial diversity

Fluid samples from both sites were dominated by sequences belonging to the *Epsilonproteobacteria* (Fig. 3). In particular, *Sulfurovum* (OTU1), a genus of mesophilic, autotrophic, and sulfide- and hydrogen-oxidizing bacteria, represented up to 37% of the sequences at Von Damm and up to 23% at Piccard. However, distinct lineages within this genus were found at each site. Four OTUs belonging to *Sulfurovum* (OTU2, OTU10, OTU21 and OTU24) were abundant at Piccard, but these OTUs were very rarely observed at Von Damm. In contrast, *Sulfurovum* OTU16 was abundant at Von Damm (up to 5%), but it was not observed at Piccard. Similar patterns were seen within the thermophilic, hydrogen-utilizing, sulfur-reducing *Epsilonproteobacteria* of the genus *Nautilia*. OTU3 was abundant at both sites, while OTU40 was only observed at Von Damm (Fig. 3).

Among the *Gammaproteobacteria*, sequences belonging to the oil-degrading genus *Alcanivorax* (OTU 9) were highly abundant at Von Damm (up to 47% at Ravelin #2), but rarely detected at Piccard (Fig. 3). Conversely, sequences belonging to the deep-sea genus *Idiomarina* (OTU 6) were abundant in vent fluids from Piccard (up to 22% at Hot Chimlet), but infrequently detected at Von Damm. The two Fuzzy Rocks samples had a taxonomic composition distinct from venting fluids and seawater (Fig. S4), and both were dominated by sequences belonging to the *Candidatus* phylum *Marithrix* (OTU0; nomenclature from Salman *et al*., 2011) within the *Thiotrichaceae* family of sulfur-oxidizing bacteria (Fig. 3), a group common in cold seeps, mud volcanoes and hydrothermal vents (Kalanetra and Nelson, 2010; Grünke *et al*., 2012; Salman *et al*., 2012). Finally, sequences related to the sulfate-reducing family *Desulfobulbaceae* within the *Deltaproteobacteria* were also found to be relatively abundant (more than 7.5%) at Shrimp Hole at Von Damm, and were extremely rare at other vents.

Overall, statistical analyses revealed a clear distinction in the microbial community structure between the two sites, with individual communities at each vent field being more similar to neighbouring orifices than to orifices at the other vent field (Fig. 4, Fig. S6). An ANalysis Of SIMilarities (ANOSIM) test indicated that groupings by vent field (Von Damm versus Piccard) were significantly different ($P = 0.001$) with respect to bacterial and archaeal community structure ($R = 0.715$ and $R = 0.683$ respectively). Oligotyping of the three dominant groups – *Methanothermococcus*, *Archaeoglobus* and *Sulfurovum* – showed identical patterns to 16S rRNA gene 96% OTUs (data not shown). Furthermore, intra-field microbial community variation was strikingly reduced at Piccard while more variation was observed at Von Damm (Fig. 4, Fig. S6). The archaeal community in a number of vents at

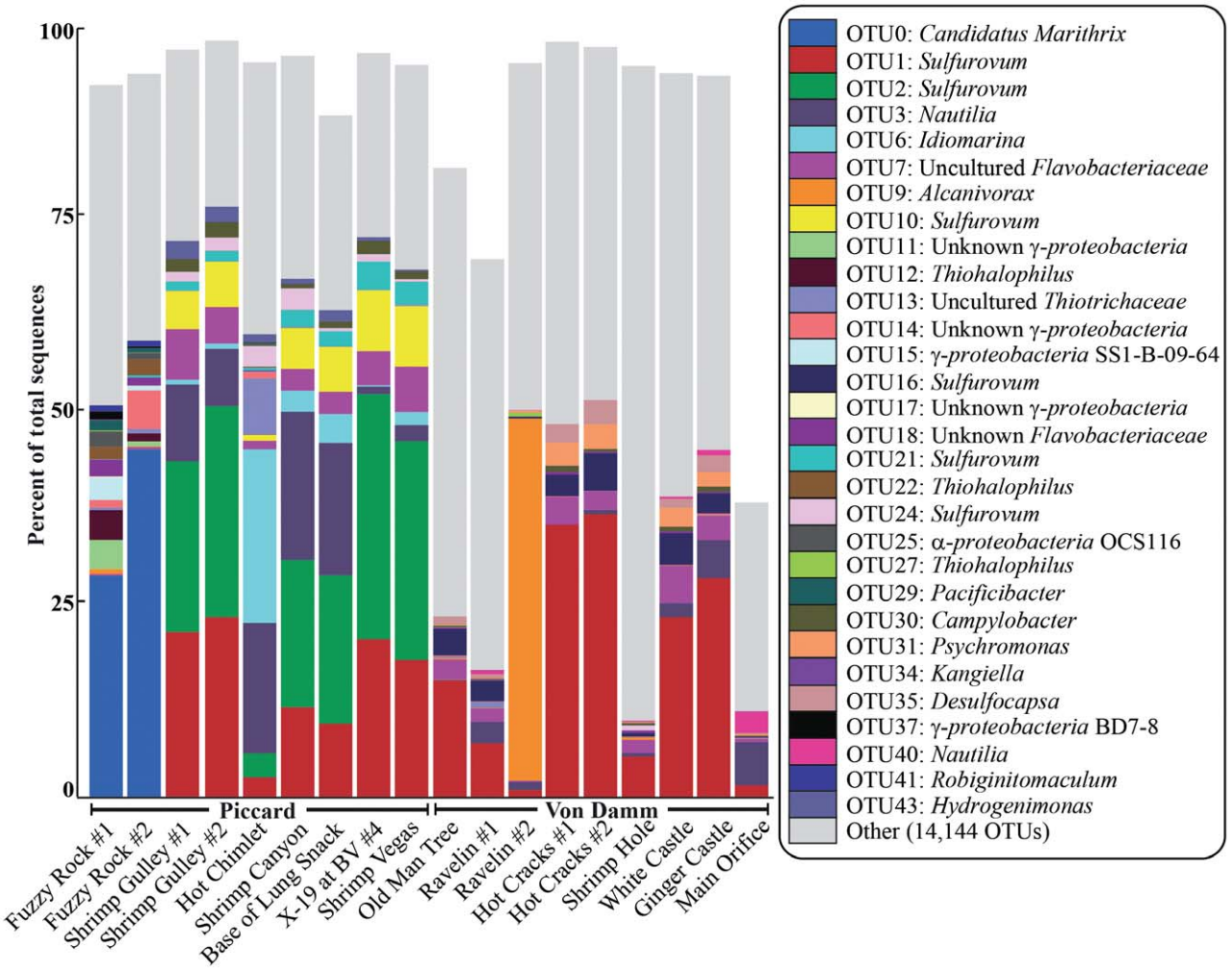

Fig. 3. Relative abundance of dominant bacterial 96% OTUs and their taxonomic assignment for rock and vent fluid samples from Piccard and Von Damm. The 30 most dominant OTUs are shown, while the others are collapsed into 'Other.'.

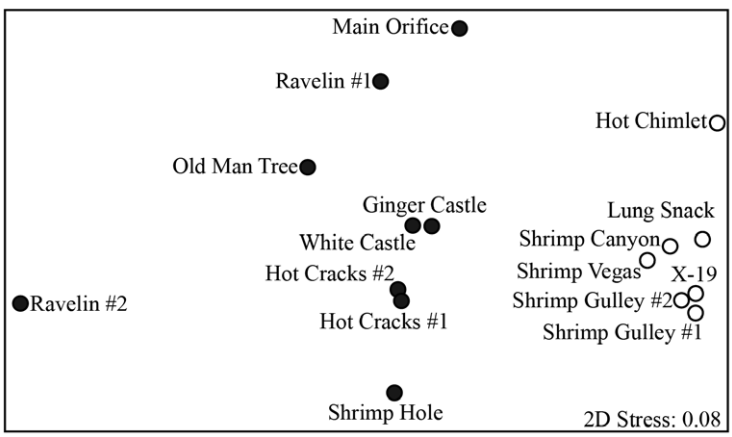

Fig. 4. MDS (multidimensional scaling) 2D similarity plot comparing 96% OTUs of bacteria, with each sample labelled according to vent field (Von Damm, filled circles; Piccard, open circles) and site name.

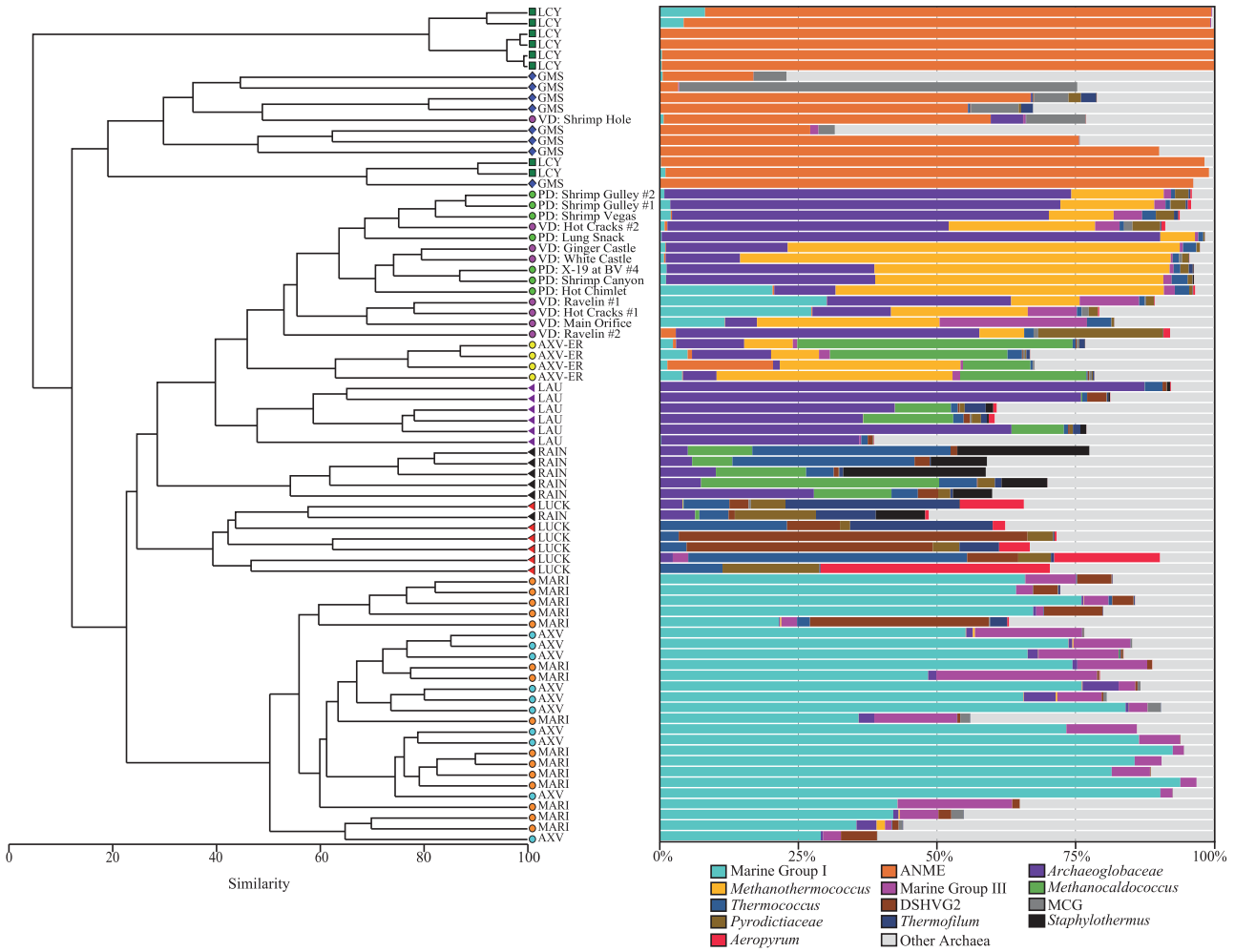

Fig. 5. Cluster diagrams of community similarity based on taxonomy of archaea at the genus level (left) and taxonomic diversity of archaeal communities (right) for Piccard (PD), Von Damm (VD), Lau Basin sulfide chimneys (LAU), the Mid-Atlantic Ridge sulfide chimneys at Rainbow (RAIN) and Lucky Strike (LUCKY), Axial diffuse vent fluids (AXV) and post-eruption 'snowblower' vent fluids (AXV-ER), Lost City carbonate chimneys (LCY), Guaymas Basin hydrothermal sediments (GMS), and Mariana Arc diffuse vent fluids (MARIANA).

Von Damm, including Shrimp Hole, Ravelin #2 and Main Orifice, showed the most compositional variability compared with the other vents from the same vent field. Ravelin #2 has extremely low magnesium concentration (Table 1), indicating a higher proportion of end-member fluid (~ 75%). ANOSIM analysis indicated that bacterial communities at orifices with a high fraction of end-member fluid (magnesium < 20 mM) were significantly different ($P = 0.008$, $R = 0.658$) from those with a low fraction of end-member fluid (magnesium > 20 mM). On the other hand, no significant grouping (in either the bacterial or the archaeal dataset) was found based on other chemical parameters, including temperature, pH, H_2S and silica. Finally, rarefaction analysis was used to compare OTU richness across all vent fluid samples. Results indicate that overall, richness was higher at Von Damm than Piccard, particularly within the archaea (Fig. S7), and that bacterial richness is an order of magnitude greater than archaeal diversity at both sites (Fig. S8).

16S rRNA global taxonomic comparisons

Taxonomic profiles of the 16S rRNA gene V6 tag sequencing data generated from Piccard and Von Damm vent fluids in this study were compared with taxonomic profiles of microbial communities from deep-sea hydrothermal vent fluids, chimneys and sediments worldwide. Community similarity analysis indicated that the MCR samples clustered together at over 50% similarity, with less than 40% similarity to all other vent sites (Fig. 5, Fig. S9). The exception is Shrimp Hole from Von Damm, which clustered with archaea from Guaymas Basin. Post-eruption 'snowblower' vents from Axial Seamount cluster at more than 40% to the MCR vent sites, although all

non-eruptive associated diffuse vents from Axial group with vents from the Mariana Arc to the exclusion of all other sites. Chimneys from Lucky Strike and Rainbow group together, distinct from Lau Basin sulfide chimneys, which are more similar to the MCR and Axial post-eruption vents than the Mid-Atlantic Ridge chimneys. Guaymas and Lost City sites cluster separately from all other samples at a very low level of similarity. Within the archaea, *Archaeoglobaceae* were dominant at both MCR vents and the Lau Basin sulfide chimneys samples, while *Methanothermococcus* were present at high relative abundance in both the MCR and the Axial 'snowblower' vents (Fig. 5). Guaymas and Lost City vents were dominated by ANME. Sequences belonging to the genus *Sulfurovum* were detected in almost all datasets, although they were strikingly abundant at the MCR (up to 79% of total bacterial sequences), and to a lower extent in Axial 'snowblower' vents, as well as Rainbow and Lau Basin sulfide chimneys (Fig. S9). Because seawater populations could possibly influence data clustering, these organisms were removed from the analysis to the best of our abilities based on taxonomic assignments and the analysis repeated; the same general patterns were seen for the MCR (data not shown).

Metagenomics

Ginger Castle from Von Damm and Shrimp Gulley #2 from Piccard were selected as representative samples from each site based on their microbial community structure inferred from V6 amplicon data (Figs 2–4) for shotgun sequencing of total community DNA. Shotgun sequencing of total community DNA yielded a total of 71 194 788 and 96 403 445 high-quality sequences for Ginger Castle (Von Damm) and Shrimp Gulley #2 (Piccard), hereafter referred to as 'Von Damm' and 'Piccard' respectively. A total of ~ 58 MB and ~ 64 MB were incorporated into contigs, yielding a total of 15 822 contigs > 2 kb (average contig length = 3664 bp; max contig length = 50 197 bp) for Von Damm and 14 239 contigs > 2 kb (average contig length = 4487 bp; maximum length = 56 073 bp) for Piccard. The total number of annotations (COGs) ranged from 2444 in Piccard to 2903 in Von Damm, and the total number of KEGGs annotations was 1619 in Piccard and 1869 in Von Damm. Alpha diversity analyses based on functional annotations show higher alpha diversity in Von Damm (Fig. S10). Taxonomic profiles of 16S rRNA genes extracted from the metagenomes were consistent with 16S rRNA gene V6 profiles, showing the dominance of *Sulfurovum* in bacteria and both *Methanothermococcus* and *Archaeoglobus* in the archaea (Fig. S11), as were the taxonomic assignments of KEGG annotations at the class level (Fig. S12), which highlighted the prevalence of *Epsilonproteobacteria*, *Archaeoglobi* and *Methanococci*. In addition, the relative abundance of archaea and bacteria from the 16S rRNA gene and KEGG metagenome annotations was consistent with quantitative PCR assays, with bacteria making up to 99% of the community at Shrimp Gulley (< 1% archaea) and 90% of the community at Ginger Castle (10% archaea) (data not shown).

The relative abundance of best hits assigned to each major subsystem (orthologous gene classes) in the two samples indicated that both sites had a similar functional profile (Fig. S13), with 'amino acid transport and metabolism', 'translation, ribosomal structure and biogenesis', and 'Energy production and conversion' dominating the general functions in both metagenomic datasets. Consistent with the COG analysis, functional gene annotation based on KEGG annotation scheme showed that both samples were very similar (Fig. S14). When examining the 20 most abundant functions in each sample, 10 were shared between both (see Fig. S15A and B), and these are represented by constitutive genes involved in the replication, recombination and repair of DNA, or in post-translational modification. Among those genes differently abundant between the two samples, the amino acid metabolism function 5-methyltetrahydrofolate-homocysteine methyltransferase (metH, MTR) was specifically enriched at Von Damm, while the functions asparagine synthetase (glutamine-hydrolysing) (asnB, ASNS) and alanyl-tRNA synthetase (AARS, alaS) were more enriched at Piccard. An assessment of the relative abundance of key genes involved in hydrogen, methane, nitrogen, sulfur and oxygen metabolism at Von Damm and Piccard showed little differences between the two sites (Fig. 6), with the exception of three genes involved in methane and hydrogen metabolism that were only detected at Von Damm. Similarly, the abundance of key genes involved in carbon fixation were similar between the two sites, with most in higher abundance at Von Damm than Piccard (Fig. 6). Finally, taxonomic assignments of these metabolic and carbon fixation genes are consistent with V6 data, with Von Damm having more different types of bacteria and archaea as compared with Piccard (Fig. S12).

Discussion

The discovery of the Piccard and Von Damm hydrothermal systems not only adds to the range of physical and chemical conditions known to support subseafloor microbial life, but also allows us to test thermodynamic predictions and compare them with both phylogenetic and functional microbial data from the same mixed fluids used in our expanded modelling effort. Given the fact that we cannot directly sample the subseafloor environment in active, unsedimented hydrothermal systems, but instead are sampling a mixture of habitats and fluids at the

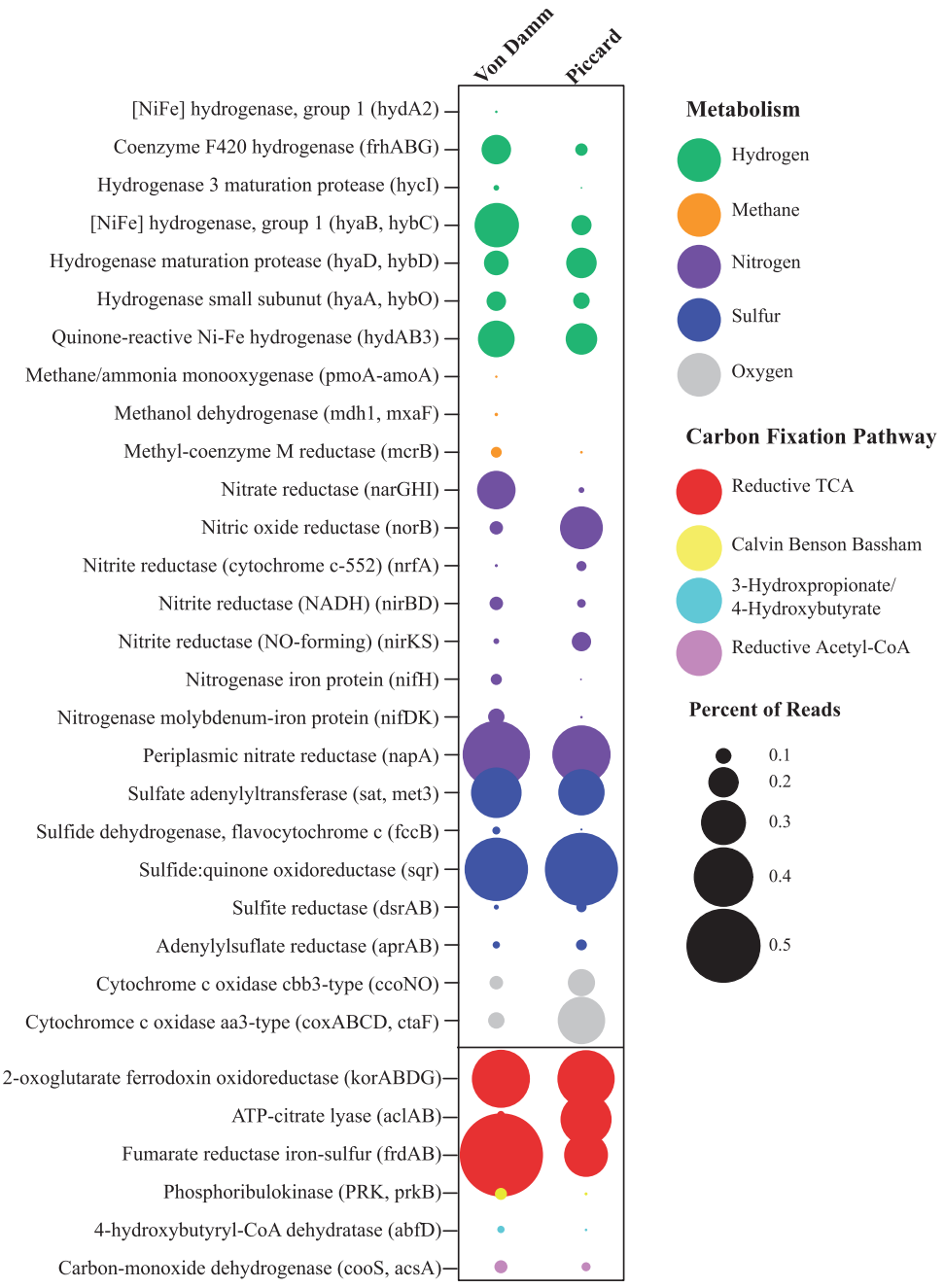

Fig. 6. Abundance of key genes involved in hydrogen, methane, nitrogen, sulfur and oxygen metabolism (above) and in carbon fixation (below) at Von Damm and Piccard.

seafloor, we used an integrative approach including chemical measurements, energetic modelling, stable isotope tracing and -omics data to infer the microbially mediated processes occurring beneath the seafloor.

Previous thermodynamic modelling efforts have suggested that ultramafic systems will host more diverse microbial communities compared with their mafic counterparts due to higher concentrations of hydrogen and reduced carbon species (McCollom, 2007; Amend *et al.*, 2011). Our modelling results show that despite the large differences in host-rock, depth, and end-member fluid temperature and geochemistry between Von Damm and Piccard, the catabolic energies available for key redox reactions are very similar, with the only difference being more energy yield for methane-based metabolisms at Von Damm. While mafic-hosted systems with extremely high

hydrogen concentrations were not included in previous modelling nor yet identified in field efforts, the present work supports the critical role of hydrogen in determining microbial community composition at deep-sea hydrothermal vents in both mafic and ultramafic-influenced hydrothermal sites. Moreover, it emphasizes the importance of temperature and pressure in regulating the composition of hydrothermal fluids that regulate chemical environments inhabited by microbial ecosystems and the inability to predict microbial community composition from rock host type alone. Our study also substantiates conclusions from previous modelling efforts (McCollom, 2007; Takai and Nakamura, 2010; Amend *et al*., 2011; Nakamura and Takai, 2014) that ultramafic systems will host more diverse lineages and metabolic functions compared with mafic counterparts due to elevated concentrations of methane. However, despite these differences in energy yields and diversity, the microbial communities at both sites show a high level of similarity, both functionally and phylogenetically, and are distinct compared with other hydrothermal systems on Earth.

At Von Damm and Piccard, both V6 amplicon and metagenomic analyses indicate that lineages within highly conserved genera of microbes, e.g. *Methanothermococcus*, *Archaeoglobus* and *Sulfurovum*, are important in the subseafloor at MCR. These three predominant genera have representative cultivars that are all capable of using hydrogen, and our metagenomic analysis shows the presence of diverse hydrogenases as well. The fact that these organisms dominate in both settings is consistent with the high concentrations of hydrogen in vent fluids at Von Damm and Piccard and the important role of hydrogen in microbial metabolism. Despite these similarities, however, at the fine scale of analysis allowed by Illumina sequencing of the V6 region, we showed that while a few OTUs were found at both sites (OTU0 in the archaea, *Archaeoglobaceae*, and OTU1 in the bacteria, *Sulfurovum*), most of the other phylotypes were found almost exclusively at only one site, with individual orifices at each vent field being more similar to each other than to orifices at the other vent field. These results show there are distinct communities of subseafloor microorganisms at both Piccard and Von Damm, and either environmental selection (fluid chemistry, pressure, temperature) or physical separation (depth, geographic distance, limits to dispersal, genetic drift), or a combination of both, has allowed for fine-scale phylogenetic differentiation of these communities. Differences in methanogenic activity were also detected between the two sites. The stable isotope tracing experiments showed methanogenesis with formate occurring at Von Damm, but not at Piccard. This result is consistent with thermodynamic models for carbon speciation that predicts higher formate concentrations at Von Damm mixed fluids relative to Piccard (Seewald *et al*., 2006; McDermott, 2014). The thermodynamic predictions have been confirmed by formate measurements in mixed fluids that indicate concentrations up to 669 μmol kg^{-1} at Von Damm and substantially lower concentration at Piccard (max 58.1 μmol kg^{-1} at Hot Chimlet; McDermott *et al*., 2015). Formate concentrations up to 158 μmol kg^{-1} have also been measured at the ultramafic site Lost City, although whether or not microorganisms are using formate at Lost City has not been demonstrated (Lang *et al*., 2010). The high methane concentrations (up to 2.8 mM in end-member fluids; Bennett *et al*., 2013; Reeves *et al*., 2014; McDermott *et al*., 2015) and potentially other reduced carbon sources at the ultramafic-influenced Von Damm vent field (Bennett *et al*., 2015; McDermott *et al*., 2015) also likely account for the greater diversity in both domains and functions relative to Piccard. While microbial communities at all Piccard vents were highly similar to one another, much more variability and diversity were observed among the vents at Von Damm. In addition, within Von Damm, there were a number of vents that looked extremely different from Piccard and other vents at Von Damm, such as Shrimp Hole, where the microbial composition was similar to those observed in cold seep sediments. Shrimp Hole is the only location at Von Damm where live tube worms were seen (Plouviez *et al*., 2015), and both genera of tube worms found (*Escarpia* and *Lamellibrachia*) have been reported in sedimented hot vents and cold methane seeps (Black *et al*., 1997). At Shrimp Hole, the archaeal population was dominated by sequences related to the unknown *Methanosarcinales* GOM Arc I group, previously described from sediments overlying a hypersaline methane seep in the Gulf of Mexico (Lloyd *et al*., 2006). In the bacterial community at Shrimp Hole, the most abundant sequence found was related to the propionate-oxidizing family *Desulfobulbaceae* within the *Deltaproteobacteria*, a frequently encountered group at methane-rich sediments and in consortia with ANME (Niemann *et al*., 2006). The high relative abundance of putative sulfate-reducing bacteria at Shrimp Hole is consistent with sulfur isotope data from this site, indicating that microbial sulfate reduction is occurring in the shallow subseafloor (Bennett *et al*., 2015). Anaerobic methane-oxidizing archaea were also frequently detected at Von Damm, including Shrimp Hole, but very rarely at Piccard. This is consistent with geochemical modelling results, where the anaerobic oxidation of methane is predicted to be moderately exergonic in ultramafic systems, but not in mafic systems (Amend *et al*., 2011, this study). The ANME lineages at Von Damm are not the same as those seen at Lost City, where a single phylotype of archaea known as the Lost City *Methanosarcinales* dominates (Schrenk *et al*., 2004). The presence of ANME and sulfate-reducing bacteria in the venting fluids at Shrimp Hole suggests seep-like characteristics (i.e. warm fluids with high

methane concentrations and high activity of anaerobic methane oxidizers) on the outer perimeter of the Von Damm vent field, similar to 'hydrothermal seeps' seen along the Costa Rica Margin, for example (Levin *et al*., 2012).

While our metagenomic work was consistent with conclusions from the V6 data with respect to both the dominant lineages and the diversity of lineages at each site, it also allowed further insight into the potential metabolisms of these communities. Our analysis revealed near functional equivalence among dominant lineages at Von Damm and Piccard based on major subsystems, as well as key hydrogen, sulfur, methane and carbon fixation genes. However, direct comparison of the thermodynamic modelling and functional profiles indicates a number of discrepancies, where the prediction from modelling does not appear consistent with the relative abundance of a particular metabolic gene. For example, specific genes involved in methanogenesis and sulfate reduction, mcr and dsr, respectively, were found in both metagenomes at relatively low abundance, although our thermodynamic modelling shows anaerobic hydrogenotrophic metabolisms should be favoured. These discrepancies can be explained by a number of important points in comparing modelling and metagenomics. First, metagenomics only highlight the functional potential, not necessarily genes that are transcribed, which is in contrast to the thermodynamic modelling, which predicts what metabolisms are most likely to be active given the energy yields under different mixing regimes, and thus temperatures. Second, our thermodynamic modelling shows these anaerobic metabolisms are favoured at 80°C under anoxic conditions, which is not the condition at the point of sampling due to mixing with seawater. Beneath the seafloor at some uncharacterized depth, these organisms are likely thriving in anoxic warm niches, where methanogenesis and sulfate reduction might be favoured. Finally, it is important to note that archaea only make up 1–10% of the microbial community in these mixed fluids, as shown by qPCR data and the extraction of 16S rRNA genes from the metagenomes, which might also explain the low abundance of these archaeal genes in the studied metagenomes. Similarly, sqr and nap, key genes involved in sulfide oxidation and nitrate reduction, respectively, are the most frequently detected reads in the metagenomes, with most mapping to *Epsilonproteobacteria*. However, thermodynamic modelling suggests that the catabolic energies available from sulfide oxidation and hydrogen denitrification are relatively low. A number of *Epsilonproteobacteria* are known to carry genes for both sulfide and hydrogen oxidation, together with nitrate reduction, such as in the genome of *Sulfurovum NBC37-1* where six copies of the sqr gene, one copy of napA and three different [Ni-Fe] hydrogenases were found (Nakagawa *et al*., 2007; Meyer and Huber, 2014). Our analysis of taxonomic annotation for each gene highlights that *Sulfurovum* at MCR have the genomic potential to carry out both sulfide and hydrogen oxidation, as well as denitrification, confirming their metabolic flexibility, even though we cannot say which metabolisms they are using at MCR.

Despite these discrepancies between the thermodynamic modelling and metagenomics analysis, overall, they are consistent with both the amplicon data and modelling efforts. Genes for all the modelled metabolisms were identified in the metagenomes, including a wide range of genes involved in hydrogen, sulfur and methane metabolism. Importantly, metabolisms that were not predicted based on modelling efforts were not seen at the level of sequencing carried out. For example, thermodynamic modelling predicted very little methane oxidation at Piccard, and this was also seen in the metagenome, with the methanol dehydrogenase and methane monooxygenases genes only found at Von Damm, not Piccard. The combined modelling and -omics effort of this study will provide the groundwork for future work focusing on *in situ* activity of organisms that will improve our understanding of which organisms and metabolisms are 'turned on' under subseafloor-relevant conditions.

In addition to comparing thermodynamic predictions to real field data from venting fluids at MCR, we also compared the newly discovered vents to sites across the globe. With the exception of Shrimp Hole, the global taxonomic analysis showed that the MCR vents are more closely related to one another than any other vent site, highlighting their distinct community structure, and the inability of only rock-host type or vent fluid chemistry to predict microbial community composition. While there are certainly weaknesses to using only taxonomic profiles rather than more sensitive techniques such as OTUs or oligotypes to compare communities, results clearly show which dominant taxa are driving differentiation among sites. For example, the MCR vents were more similar to eruption-associated ephemeral diffuse vents than to any other environment surveyed due to high relative abundance of *Methanothermococcus* and *Sulfurovum*. Meyer and colleagues (2013) suggest these anaerobic methanogens and other microaerobic taxa in Axial snowblower come from deeper communities that are seeded from the volatile-rich eruptive fluids, which could explain the high level of microbial community similarity between Axial snowblower vents and the hot and reduced MCR vent fluids. Similarly, the high abundance of hyperthermophilic sulfate reducers *Archeaglobaceae*, commonly found in sulfide chimneys, where sulfate and either organics or hydrogen are provided by seawater and hot fluids, respectively, supports the high similarity level between sulfide chimneys of Lau Basin and the MCR samples. Interestingly, the two ultramafic sites with similarly high concentrations of hydrogen to Von

Damm and Piccard – Rainbow with 12–16 mM end-member hydrogen (Charlou *et al*., 2002) and Lost City with ~ 10 mM hydrogen (Kelley *et al*., 2002) – showed distinct lineages not found at the MCR vents, including *Methanocaldococcus* at Rainbow, novel ANME lineages at Lost City, and *Thiomicrospira* at both. In line with these findings, the analysis also showed that sequences of the Epsilonproteobacterial group, *Sulfurovum*, the key bacteria in the MCR, have not been detected in such abundance in any other hydrothermal systems. Bacterial communities in fluids from volcanoes of the Mariana Arc and Axial Seamount are dominated by the aerobic or microaerobic, mesophilic group *Sulfurimonas*. These frequently detected lineages in diffuse fluids are also found in hydrothermal sediments (Inagaki, 2003), associated with vent animals (Takai *et al*., 2006), in coastal marine sediments (Sievert *et al*., 2008), and in redox clines (Grote *et al*., 2012), but were strikingly absent in MCR fluids. Similarly, the *Gammaproteobacteria* lineage SUP05, an ubiquitous deep ocean aerobic sulfur-oxidizing bacterium that is abundant in other vent environments (Anantharaman *et al*., 2012; Akerman *et al*., 2013; Anderson *et al*., 2013; Dick *et al*., 2013) were not detected at the MCR. The absence of both of these lineages is likely attributed to the highly reducing nature of the MCR vent sites, as well as the elevated temperatures of mixed fluids. Consistent with thermodynamic predictions, at temperatures above ~ 40°C, the (micro)aerobic metabolisms of these psychrophilic or moderately mesophilic groups are not expected. This comparison of microbial taxonomic profiles across different deep-sea hydrothermal vent environments, spanning a wide diversity of systems from ephemeral eruptive hydrothermal events to sulfide chimneys at the global scale, confirms the distinct composition and structure of the MCR subseafloor microbial communities. Altogether, these findings from the newly discovered MCR vent fields represent an important advance in the field of hydrothermal and subseafloor research, shedding light on new aspects of diversity for venting types, fluid chemistry and subseafloor microbial communities along the spectrum of known volcanism on our planet.

Experimental procedures

Sample collection and chemical measurements

Low temperature diffuse hydrothermal fluid samples were collected in January 2012 using the ROV Jason II (Table S1) and the Mat Sampler, as described in Breier and colleagues (2012). This involved measuring the fluid temperature with the Jason temperature probe in regions of hydrothermal fluid flow (Fig. S2), then positioning the sampler intake into the vent and pumping fluid through either a 0.22 μm Sterivex™-GP filter (Millipore) or a custom-made non-gas-tight 100 ml flow-through water bottle. For filter samples, at least 2 l of fluid were filtered at a flow rate of < 0.2 l per minute. For whole water samples collected in bottles, fluids were pumped at 1 l per minute until at least 3 l of fluid flushed the bottle. To minimize cross-contamination potential, each sample container had its own sample inlet and pumping line.

Upon vehicle recovery, filters were flooded with RNALater, sealed with Male/Female Luer Caps, and stored in sterile Falcon tubes. Filters were stored at 4 °C for 18–24 h before being stored at −80°C until nucleic acid extraction in the laboratory. Fluids were analysed shipboard for pH (25°C, 1 atm) using an Ag/AgCl combination reference electrode and for dissolved total sulfide (ΣH_2S) by iodometric titration of triplicate aliquots drawn into syringes. The 2σ analytical uncertainties were ±0.05 for pH and ±10% for H_2S. Dissolved magnesium and silica were analysed by inductively coupled plasma-mass spectrometry on land (2σ of 5% for both).

Collection and analysis of background seawater and rock samples are described in the *Supporting information*.

Cell counts and cultivation

Vent fluid samples were preserved in formaldehyde for total cell enumeration using epifluorescence microscopy with DAPI, as described previously (Breier *et al*., 2012).

Stable isotope tracer experiments

Vent fluids were also used in stable isotope tracing incubation experiments containing ^{13}C-labelled sodium bicarbonate and ^{13}C-labelled sodium formate (Cambridge Isotopes). These experiments were conducted shipboard immediately after sample collection. Of the vent fluid, 3 ml was added to a 7 ml Exetainer (Labco Limited, High Wycombe, Buckinghamshire, UK) containing a total concentration of 1 mM substrate (1% labelled). All Exetainers were prepared in an anaerobic chamber, flushed with nitrogen, and capped with a butyl rubber stopper and screw cap. Each labelled experiment was carried out in triplicate plus one filter-sterilized negative control. Exetainers were incubated at 70°C for ~ 72 h, then injected with 0.2 ml of 85% phosphoric acid. Tubes were stored upside down and transported at room temperature. One millilitre of 50% NaOH was added to each tube before analysing CH_4 $^{13}C/^{12}C$ ratios using a Thermo-Finnigan Delta Plus XL Isotope Ratio Mass Spectrometer coupled to an Agilent 6890 Gas Chromatograph via a GCIII combustion interface.

DNA extraction, V6 polymerase chain reaction (PCR) and Illumina tag sequencing

After thawing filters to room temperature, total genomic DNA was extracted from vent fluids and seawater as previously described in Akerman and colleagues (2013). Total genomic DNA from microbial filaments on rock samples was extracted using the MoBio UltraClean Soil DNA Isolation Kit. DNA was quantified with PicoGreen (Life Technologies) on a Turner Biosystems spectrophotometer. Hypervariable region six (V6) of the 16S rRNA gene (*ca*. 60 nucleotides) was PCR amplified in triplicate for each sample for bacteria and archaea separately according to Eren and colleagues (2013). Genomic DNA from the rock samples was PCR amplified for

bacteria only. Triplicate PCR products for each sample were pooled, cleaned using the Qiagen MinElute Kit (Qiagen, Valencia, CA), and quantified with PicoGreen (Life Technologies). Samples were then pooled and sequenced according to Meyer and colleagues (2013).

V6 Processing, data analysis and global taxonomic comparisons

Sequence quality trimming and filtering were based on paired-end reads overlap analysis of Illumina sequence reads, as described in Eren and colleagues (2013) and the *Supporting information*. Oligotyping analysis is also described in the *Supporting information*. Quality-filtered V6 reads are publicly available through the VAMPS database (https://vamps.mbl.edu) under the projects JAH_MCR_Av6 and JAH_MCR_Bv6. Raw reads for V6 are available in the NCBI Short Read Archive under Accession Number PRJNA258374. Given the focus of this study on subseafloor organisms and the dramatic differences in depth between the two sites, we distinguished vent-specific microbial communities from background seawater communities that mix with venting fluids at the point of sampling or in the shallow seafloor by removing 16S rRNA gene operational taxonomic units (OTUs) that also occurred in seawater (Niskin samples at more than 0.005% of the reads after normalization) from each fluid sample prior to further analyses. Statistical analyses are described in the *Supporting information*. The 16S rRNA archaeal and bacterial data from this study were also compared with those from previous studies, and the details of that analysis are provided in the *Supporting information*.

16S rRNA gene amplification, cloning and sequencing

Full-length archaeal 16S rRNA genes were PCR amplified on an Eppendorf thermal cycler using the primers ARC-8F (5′-TCCGGTTGATCCTGCC-3′) and ARC-1492R (5′-GG CTACCTTGTTACGACTT-3′) on DNA from Hot Cracks #2 and Base of Lung Snack fluid samples collected at Von Damm and Piccard, respectively, as described in the *Supporting information*. Representative clone sequences are available at NCBI under accession numbers KJ622295-KJ622297.

Quantitative PCR (qPCR)

The qPCR probe-based assays described previously (Takai and Horikoshi, 2000; Nadkarni *et al*., 2002) were used to determine the relative abundance of bacterial and archaeal 16S rRNA genes in vent fluids, as described in Huber and colleagues (2010) and the *Supporting information*. Copy numbers were normalized using a conversion of 4.1 or 1.6 copies per cell for bacteria or archaea respectively (Klappenbach *et al*., 2001).

Energetic modelling

An equilibrium thermodynamic reaction path model was used to calculate the free energy available from eight different types of metabolism – sulfide oxidation, methane oxidation, iron oxidation, aerobic hydrogen oxidation, sulfate reduction, methanogenesis, anaerobic methane oxidation and denitrification – in order to assess the potential for chemoautotrophic metabolisms at both the Von Damm and Piccard vents. We compared these two sites using end-member geochemical data from Reeves and colleagues (2014) and McDermott and colleagues (2015) with six vents previously analysed by Amend and colleagues (2011), three of which are basalt-hosted vents (EPR 21°N, Lucky Strike and TAG) and three of which are peridotite-influenced vents (Lost City, Logatchev and Rainbow). A detailed description of the modelling approach is provided in the *Supporting information*.

Metagenomics

Ginger Castle from Von Damm and Shrimp Gulley #2 from Piccard were analysed for shotgun sequencing of total community DNA. DNA was sheared to 175 bp using a Covaris S-series sonicator, and metagenomic library construction was completed using the Ovation Ultralow Library DR multiplex system (Nugen) following manufacturer's instructions. Metagenomic sequencing was performed on an Illumina HiSeq 1000 at the W.M. Keck sequencing facility at the Marine Biological Laboratory. All libraries were paired-end, with a 30 bp overlap, resulting in an average merged read length of 170 bp. Sequence quality trimming and filtering relied upon perfect identity of paired-end read overlaps using the Illumina-utils libraries, as described in Eren and colleagues (2013). The two metagenomic datasets were assembled using CLC Genomics Workbench 4.9. Assembled contigs were submitted to the DOE Joint Genome Institutes (JGI) for gene calling and functional annotation, where protein coding genes are associated with Pfams, COGs, KO terms, EC numbers and phylogeny. Reads were mapped on the open reading frames identified with JGI using Bowtie 2 (Langmead and Salzberg, 2012) in order to obtain the abundance of each functional assignment. The abundance of individual reads matching a particular cluster of orthologous genes (COGs) were normalized by the average abundance of 38 single copy COGs genes as described in Fan and colleagues (2012). This approach provided a proxy for the number of genomes harbouring a specific COG in the community and was used to generate a metabolic profile of the two metagenomes. The abundance of reads matching a particular KEGG was normalized to RNA polymerase beta subunit (rpoB) gene counts. An expectation value threshold of 1e-10 was applied. Only hits with greater than 30% identity of aligned amino acid residues and alignment length of 30 amino acids (*ca.* a third of the average length of a prokaryote gene) were considered for the analysis. 16S RNA gene sequences were also extracted from metagenomes, as described in the *Supporting information*. Heat maps were created using R. In order to estimate and visualize alpha diversity in the metagenomic samples, the frequency of reads functional annotation was calculated as a function of their occurrence (including log scale) using in-house R scripts. We used the R library ggplot version 1.0.1 for visualization of the gene's taxonomic assignments. The metagenome raw reads are available in the European Nucleotide Archive under Study Accession Number PRJEB9204 (http://www.ebi.ac.uk/ena/data/view/PRJEB9204).

Acknowledgements

This work was supported through funding from the National Aeronautics and Space Administration (NASA) Astrobiology Science and Technology for Exploring Planets grant (NNX09AB756) to JAH, CRG and JS, the Deep Carbon Observatory's Deep Life I grant to JAH, which is supported by the Alfred P. Sloan Foundation. Ship and vehicle time were supported via NSF Award OCE106183 to CRG and JS. Chip Breier and the crews of the ROV Jason II and R/V Atlantis provided critical support during cruise planning, at sea operations, and post-cruise analysis and interpretation. Caroline Fortunato provided important feedback during manuscript preparation and data analysis. Hilary Morrison provided assistance with data sequencing and archiving. Richard Fox, Loïs Maignien and A. Murat Eren provided support with the use of MBL supercomputers and R and ggplot libraries respectively. Comments from two anonymous reviewers greatly improved the final version of this manuscript. This is C-DEBI contribution 282. The authors declare they have no conflict of interest.

References

Akerman, N.H., Butterfield, D.A., and Huber, J.A. (2013) Phylogenetic diversity and functional gene patterns of sulfur-oxidizing subseafloor Epsilonproteobacteria in diffuse hydrothermal vent fluids. *Front Microbiol* **4:** 185.

Amend, J.P., McCollom, T.M., Hentscher, M., and Bach, W. (2011) Catabolic and anabolic energy for chemolithoautotrophs in deep-sea hydrothermal systems hosted in different rock types. *Geochim Cosmochim Acta* **75:** 5736–5748.

Anantharaman, K., Breier, J.A., Sheik, C.S., and Dick, G.J. (2012) Evidence for hydrogen oxidation and metabolic plasticity in widespread deep-sea sulfur-oxidizing bacteria. *Proc Natl Acad Sci USA* **10:** 330–335.

Anderson, R.E., Beltrán, M.T., Hallam, S.J., and Baross, J.A. (2013) Microbial community structure across fluid gradients in the Juan de Fuca Ridge hydrothermal system. *FEMS Microbiol Ecol* **83:** 324–339.

Beaulieu, S.E., Baker, E.T., German, C.R., and Maffei, A. (2013) An authoritative global database for active submarine hydrothermal vent fields. *Geochem Geophys Geosyst* **14:** 4892–4905.

Bennett, S.A., Coleman, M., Huber, J.A., Reddington, E., Kinsey, J.C., McIntyre, C., *et al*. (2013) Trophic regions of a hydrothermal plume dispersing away from an ultramafic-hosted vent-system: Von Damm vent-site, Mid-Cayman Rise. *Geochem Geophys Geosyst* **14:** 317–327.

Bennett, S.A., Van Dover, C., Breier, J.A., and Coleman, M. (2015) Effect of depth and vent fluid composition on the carbon sources at two neighboring deep-sea hydrothermal vent fields (Mid-Cayman Rise). *Deep Sea Res Part I Oceanogr Res Pap* **104:** 122–133.

Black, M.B., Halanych, K.M., Maas, P.A.Y., Hoeh, W.R., Hashimoto, J., Desbruyères, D., *et al*. (1997) Molecular systematics of vestimentiferan tubeworms from hydrothermal vents and cold-water seeps. *Mar Biol* **130:** 141–149.

Brazelton, W.J., Schrenk, M.O., Kelley, D.S., and Baross, J.A. (2006) Methane- and sulfur-metabolizing microbial communities dominate the Lost City hydrothermal field ecosystem. *Appl Environ Microbiol* **72:** 6257–6270.

Brazelton, W.J., Mehta, M.P., and Kelley, D.S. (2011) Physiological differentiation within a single-species biofilm fueled by serpentinization. *Mbio* **4:** 1–9.

Brazelton, W.J., Nelson, B., and Schrenk, M.O. (2012) Metagenomic evidence for H2 oxidation and H2 production by serpentinite-hosted subsurface microbial communities. *Front Microbiol* **2:** 268.

Brazelton, W.J., Morrill, P.L., Szponar, N., and Schrenk, M.O. (2013) Bacterial communities associated with subsurface geochemical processes in continental serpentinite springs. *Appl Environ Microbiol* **79:** 3906–3916.

Breier, J.A., Gomez-Ibanez, D., Reddington, E., Huber, J.A., and Emerson, D. (2012) A precision multi-sampler for deep-sea hydrothermal microbial mat studies. *Deep Sea Res Part I Oceanogr Res Pap* **70:** 83–90.

Chapelle, F.H., O'Neill, K., Bradley, P.M., Methé, B.A., Ciufo, S.A., Knobel, L.L., and Lovley, D.R. (2002) A hydrogen-based subsurface microbial community dominated by methanogens. *Nature* **415:** 312–315.

Charlou, J.L., Donval, J.P., Fouquet, Y., Jean-Baptiste, P., and Holm, N.G. (2002) Geochemistry of high H2 and CH4 vent fluids issuing from ultramafic rocks at the Rainbow hydrothermal field (36 140N, MAR). *Chem Geol* **191:** 345–359.

Connelly, D.P., Copley, J.T., Murton, B.J., Stansfield, K., Tyler, P.A., German, C.R., *et al*. (2012) Hydrothermal vent fields and chemosynthetic biota on the world's deepest seafloor spreading centre. *Nat Commun* **3:** 620.

Dick, G.J., Anantharaman, K., Baker, B.J., Li, M., Reed, D.C., and Sheik, C.S. (2013) The microbiology of deep-sea hydrothermal vent plumes: ecological and biogeographic linkages to seafloor and water column habitats. *Front Microbiol* **4:** 124.

Eren, A.M., Vineis, J.H., Morrison, H.G., and Sogin, M.L. (2013) A filtering method to generate high quality short reads using Illumina paired-end technology. *PLoS ONE* **8:** e66643.

Fan, L., Reynolds, D., Liu, M., Stark, M., Kjelleberg, S., and Webster, N.S. (2012) Functional equivalence and evolutionary convergence in complex communities of microbial sponge symbionts. *Proc Natl Acad Sci USA* **109:** 1878–1887.

Flores, G.E., Campbell, J.H., Kirshtein, J.D., Meneghin, J., Podar, M., Steinberg, J.I., *et al*. (2011) Microbial community structure of hydrothermal deposits from geochemically different vent fields along the Mid-Atlantic Ridge. *Environ Microbiol* **13:** 2158–2171.

German, C.R., Bowen, A., Coleman, M.L., Honig, D.L., Huber, J.A., Jakuba, M.V., *et al*. (2010) Diverse styles of submarine venting on the ultraslow spreading Mid-Cayman Rise. *Proc Natl Acad Sci USA* **107:** 14020–14025.

Grote, J., Schott, T., Bruckner, C.G., Glöckner, F.O., Jost, G., Teeling, H., *et al*. (2012) Genome and physiology of a model Epsilonproteobacterium responsible for sulfide detoxification in marine oxygen depletion zones. *Proc Natl Acad Sci USA* **109:** 506–510.

Grünke, S., Lichtschlag, A., de Beer, D., Felden, J., Salman, V., Ramette, A., *et al*. (2012) Mats of psychrophilic thiotrophic bacteria associated with cold seeps of the Barents Sea. *Biogeosciences* **9:** 2947–2960.

Huber, J.A., and Holden, J.F. (2008) Modeling the impact of diffuse vent microorganisms along mid-ocean ridges and flanks. In *Magma to Microbe*. Lowell, R.P., Seewald, J.S., Metaxas, A., and Perfit, M.R. (eds). Washington, D.C., WA, USA: American Geophysical Union, pp. 215–232.

Huber, J.A., Butterfield, D.A., and Baross, J.A. (2002) Temporal changes in archaeal diversity and chemistry in a mid-ocean ridge subseafloor habitat. *Appl Environ Microbiol* **68:** 1585–1594.

Huber, J.A., Mark Welch, D.B., Morrison, H.G., Huse, S.M., Neal, P.R., Butterfield, D.A., and Sogin, M.L. (2007) Microbial population structures in the deep marine biosphere. *Science* **318:** 97–100.

Huber, J.A., Cantin, H.V., Huse, S.M., Welch, D.B.M., Sogin, M.L., and Butterfield, D.A. (2010) Isolated communities of Epsilonproteobacteria in hydrothermal vent fluids of the Mariana Arc seamounts. *FEMS Microbiol Ecol* **73:** 538–549.

Inagaki, F., Takai, K., Kobayashi, H., Nealson, K.H., and Horikoshi, K. (2003) *Sulfurimonas autotrophica* gen. nov., sp. nov., a novel sulfur-oxidizing epsilon-proteobacterium isolated from hydrothermal sediments in the Mid-Okinawa Trough. *Int J Syst Evol Microbiol* **53:** 1801–1805.

Kalanetra, K.M., and Nelson, D.C. (2010) Vacuolate-attached filaments: highly productive *Ridgeia piscesae* epibionts at the Juan de Fuca hydrothermal vents. *Mar Biol* **157:** 791–800.

Kelley, D.S., Baross, J.A., and Delaney, J.R. (2002) Volcanoes, fluids, and life at Mid-Ocean Ridge spreading centers. *Annu Rev Earth Planet Sci* **30:** 385–491.

Kelley, D.S., Karson, J.A., Früh-Green, G.L., Yoerger, D.R., Shank, T.M., Butterfield, D.A., *et al*. (2005) A serpentinite-hosted ecosystem: the Lost City hydrothermal field. *Science* **307:** 1428–1434.

Kinsey, J.C., and German, C.R. (2013) Sustained volcanically-hosted venting at ultraslow ridges: Piccard, Hydrothermal Field, Mid-Cayman Rise. *Earth Planet Sci Lett* **380:** 162–168.

Klappenbach, J.A., Saxman, P.R., Cole, J.R., and Schmidt, T.M. (2001) rrndb: the ribosomal RNA operon copy number database. *Nucleic Acids Res* **29:** 181–184.

Lang, S.Q., Butterfield, D.A., Schulte, M., Kelley, D.S., and Lilley, M.D. (2010) Elevated concentrations of formate, acetate and dissolved organic carbon found at the Lost City hydrothermal field. *Geochim Cosmochim Acta* **74:** 941–952.

Langmead, B., and Salzberg, S.L. (2012) Fast gapped-read alignment with Bowtie 2. *Nat Methods* **9:** 357–359.

Levin, L.A., Orphan, V.J., Rouse, G.W., Rathburn, A.E., Ussler, W., III, Cook, G.S., *et al*. (2012) A hydrothermal seep on the Costa Rica margin: middle ground in a continuum of reducing ecosystems. *Proc Biol Sci* **279:** 2580–2588.

Lloyd, K.G., Lapham, L., and Teske, A. (2006) An anaerobic methane-oxidizing community of ANME-1b archaea in hypersaline Gulf of Mexico sediments. *Appl Environ Microbiol* **72:** 7218–7230.

McCollom, T.M. (2007) Geochemical constraints on sources of metabolic energy for chemolithoautotrophy in ultramafic-hosted deep-sea hydrothermal systems. *Astrobiology* **7:** 933–950.

McCollom, T.M., and Shock, E.L. (1997) Geochemical constraints on chemolithoautotrophic metabolism by microorganisms in seafloor hydrothermal systems. *Geochim Cosmochim Acta* **61:** 4375–4391.

McDermott, J.M. (2014) Geochemistry of deep-sea hydrothermal vent fluids from the Mid-Cayman Rise, Caribbean Sea. PhD thesis. Chemical Oceanography, MIT/WHOI Joint Program in Oceanography,Woods Hole, MA, USA.

McDermott, J.M., Seewald, J.S., German, C.R., and Sylva, S.P. (2015) Pathways for abiotic organic synthesis at submarine hydrothermal fields. *Proc Natl Acad Sci USA* **112:** 7668–7672.

Meyer, J.L., and Huber, J.A. (2014) Strain-level genomic variation in natural populations of Lebetimonas from an erupting deep-sea volcano. *ISME J* **8:** 867–880.

Meyer, J.L., Akerman, N.H., Proskurowski, G., and Huber, J.A. (2013) Microbiological characterization of post-eruption 'snowblower' vents at Axial Seamount, Juan de Fuca Ridge. *Front Microbiol* **4:** 153.

Nadkarni, M.A., Martin, F.E., Jacques, N.A., and Hunter, N. (2002) Determination of bacterial load by real-time PCR using a broad-range (universal) probe and primers set. *Microbiology* **148:** 257–266.

Nakagawa, S., Takaki, Y., Shimamura, S., Reysenbach, A., Takai, K., and Horikoshi, K. (2007) Deep-sea vent epsilon-proteobacterial genomes provide insights into emergence of pathogens. *Proc Natl Acad Sci USA* **104:** 12146–12150.

Nakamura, K., and Takai, K. (2014) Theoretical constraints of physical and chemical properties of hydrothermal fluids on variations in chemolithotrophic microbial communities in seafloor hydrothermal systems. *Prog Earth Planet Sci* **1:** 5.

Nealson, K.H., Inagaki, F., and Takai, K. (2005) Hydrogen-driven subsurface lithoautotrophic microbial ecosystems (SLiMEs): do they exist and why should we care? *Trends Microbiol* **13:** 405–410.

Nercessian, O., Bienvenu, N., Moreira, D., Prieur, D., and Jeanthon, C. (2005) Diversity of functional genes of methanogens, methanotrophs and sulfate reducers in deep-sea hydrothermal environments. *Environ Microbiol* **7:** 118–132.

Niemann, H., Lösekann, T., de Beer, D., Elvert, M., Nadalig, T., Knittel, K., *et al*. (2006) Novel microbial communities of the Haakon Mosby mud volcano and their role as a methane sink. *Nature* **443:** 854–858.

Nunoura, T., and Takai, K. (2009) Comparison of microbial communities associated with phase-separation-induced hydrothermal fluids at the Yonaguni Knoll IV hydrothermal field, the Southern Okinawa Trough. *FEMS Microbiol Ecol* **67:** 351–370.

Perner, M., Kuever, J., Seifert, R., Pape, T., Koschinsky, A., Schmidt, K., *et al*. (2007) The influence of ultramafic rocks on microbial communities at the Logatchev hydrothermal field, located 15 degrees N on the Mid-Atlantic Ridge. *FEMS Microbiol Ecol* **61:** 97–109.

Perner, M., Petersen, J.M., Zielinski, F., Gennerich, H.-H., and Seifert, R. (2010) Geochemical constraints on the

diversity and activity of H2-oxidizing microorganisms in diffuse hydrothermal fluids from a basalt- and an ultramafic-hosted vent. *FEMS Microbiol Ecol* **74:** 55–71.
Plouviez, S., Jacobson, A., Wu, M., and Van Dover, C.L. (2015) Characterization of vent fauna at the Mid-Cayman Spreading Center. *Deep Sea Res Part I Oceanogr Res Pap* **97:** 124–133.
Reeves, E.P., McDermott, J.M., and Seewald, J.S. (2014) The origin of methanethiol in mid-ocean ridge hydrothermal fluids. *Proc Natl Acad Sci USA* **111:** 5474–5479.
Roussel, E.G., Konn, C., Charlou, J.-L., Donval, J.P., Fouquet, Y., Querellou, J., *et al*. (2011) Comparison of microbial communities associated with three Atlantic ultramafic hydrothermal systems. *FEMS Microbiol Ecol* **77:** 647–665.
Salman, V., Amann, R., Girnth, A.-C., Polerecky, L., Bailey, J.V., Høgslund, S., *et al*. (2011) A single-cell sequencing approach to the classification of large, vacuolated sulfur bacteria. *Syst Appl Microbiol* **34:** 243–259.
Salman, V., Amann, R., Shub, D.A., and Schulz-Vogt, H.N. (2012) Multiple self-splicing introns in the 16S rRNA genes of giant sulfur bacteria. *Proc Natl Acad Sci USA* **109:** 4203–4208.
Schrenk, M.O., Kelley, D.S., Bolton, S.A., and Baross, J.A. (2004) Low archaeal diversity linked to subseafloor geochemical processes at the Lost City Hydrothermal Field, Mid-Atlantic Ridge. *Environ Microbiol* **6:** 1086–1095.
Schrenk, M.O., Brazelton, W.J., and Lang, S.Q. (2013) Serpentinization, carbon, and deep life. *Rev Miner Geochem* **75:** 575–606.
Seewald, J.S., Doherty, K.W., Hammar, T.R., and Liberatore, S.P. (2001) A new gas-tight isobaric sampler for hydrothermal fluids. *Deep Sea Res Part I Oceanogr Res Pap* **49:** 189–196.
Seewald, J.S., Zolotov, M., and McCollom, T.M. (2006) Experimental investigation of carbon speciation under hydrothermal conditions. *Geochim Cosmochim Acta* **70:** 446–460.
Sievert, S.M., Scott, K.M., Klotz, M.G., Chain, P.S.G., Hauser, L.J., Hemp, J., *et al*. (2008) Genome of the epsilonproteobacterial chemolithoautotroph *Sulfurimonas denitrificans*. *Appl Environ Microbiol* **74:** 1145–1156.
Stevens, T.O., McKinley, J.P., and Stevens, T. (1995) Lithoautotrophic microbial ecosystems in deep basalt aquifers. *Science* **270:** 450–454.
Takai, K., and Horikoshi, K. (2000) Rapid detection and quantification of members of the archaeal community by quantitative PCR using fluorogenic probes. *Appl Environ Microbiol* **66:** 5066–5072.
Takai, K., and Nakamura, K. (2010) Compositional, physiological and metabolic variability in microbial communities associated with geochemically diverse, deep-sea hydrothermal vent fluids. In *Geomicrobiology: Molecular and Environmental Perspective*. Barton, L.L., Mandl, M., and Loy, A. (eds). Dordrecht, The Netherlands: Springer, pp. 251–283.
Takai, K., Gamo, T., Tsunogai, U., Nakayama, N., Hirayama, H., Nealson, K.H., and Horikoshi, K. (2004) Geochemical and microbiological evidence for a hydrogen-based, hyperthermophilic subsurface lithoautotrophic microbial ecosystem (HyperSLiME) beneath an active deep-sea hydrothermal field. *Extremophiles* **8:** 269–282.
Takai, K., Nakamura, K., Suzuki, K., Inagaki, F., Nealson, K.H., and Kumagai, H. (2006) Ultramafics-Hydrothermalism-Hydrogenesis-HyperSLiME (UltraH3) linkage: a key insight into early microbial ecosystem in the Archean deep-sea hydrothermal systems. *Paleontol Res* **10:** 269–282.
Takai, K., Nakamura, K., Toki, T., Tsunogai, U., Miyazaki, M., Miyazaki, J., *et al*. (2008) Cell proliferation at 122 degrees C and isotopically heavy CH4 production by a hyperthermophilic methanogen under high-pressure cultivation. *Proc Natl Acad Sci USA* **105:** 10949–10954.
Ver Eecke, H.C., Butterfield, D.A., Huber, J.A., Lilley, M.D., Olson, E.J., Roe, K.K., *et al*. (2012) Hydrogen-limited growth of hyperthermophilic methanogens at deep-sea hydrothermal vents. *Proc Natl Acad Sci USA* **109:** 13674–13679.

Supporting information

Additional Supporting Information may be found in the online version of this article at the publisher's web-site:

Fig. S1. Map of Caribbean Sea, with blue diamond indicating the location of the Mid-Cayman Rise (inset). Von Damm and Piccard hydrothermal vent fields are shown in white diamonds.
Fig. S2. ROV pictures of vent fluid sampling at selected vent site locations. (A) Old Man Tree at Von Damm; (B) Shrimp Hole at Von Damm; (C) Shrimp Gulley at Piccard, Beebe Sea Mound; and (D) Fuzzy Rocks at Piccard, Beebe Vents Mound.
Fig. S3. DAPI-stained epifluorescent micrographs of microorganisms found in venting fluids at (A) Shrimp Gulley #2, Piccard; (B) White Castle, Von Damm; (C) Hot Cracks #1, Von Damm; and (D) Shrimp Hole, Von Damm. All scale bars are 2 μm.
Fig. S4. MDS (multidimensional scaling) 2D similarity plot comparing all 16S rRNA gene 96% OTUs of (A) archaea and (B) bacteria, with each sample labelled according to vent field (Von Damm, filled circles; Piccard, open circles) and site name, including background seawater (filled squares) and Fuzzy Rocks samples (open squares).
Fig. S5. Neighbour-joining tree of full-length 16S rRNA genes corresponding to Archaeglobacae sequences. Bootstrap values greater than 75 are indicated above branches. Sequences obtained in this study are highlighted in bold. The number of replicate clones is shown in parentheses.
Fig. S6. MDS 2D similarity plot comparing 16S rRNA gene 96% OTUs of archaea, with each sample labelled according to vent field (Von Damm, filled circles; Piccard, open circles) and site name. Shrimp Hole is not included in the analysis.
Fig. S7. Rarefaction curve of 16S rRNA genes at 96% OTUs of archaea at (A) Von Damm and (B) Piccard, with each sample labelled according to vent site name.
Fig. S8. Rarefaction curve of 16S rRNA genes at 96% OTUs of bacteria at (A) Von Damm and (B) Piccard, with each sample labelled according to vent site name.
Fig. S9. Cluster diagrams of community similarity based on taxonomy of bacterial 16S rRNA genes at the genus level (left) and taxonomic diversity of bacterial communities (right) for Piccard (PD), Von Damm (VD), Lau Basin sulfide chimneys (LAU), the Mid-Atlantic Ridge sulfide chimneys at

Rainbow (RAIN) and Lucky Strike (LUCKY), Axial diffuse vent fluids (AXV) and post-eruption 'snowblower' vent fluids (AXV-ER), Lost City carbonate chimneys (LCY), Guaymas Basin hydrothermal sediments (GMS), and Mariana Arc diffuse vent fluids (MARIANA).

Fig. S10. Number of KEGGs ontology as a function of (A) frequency and (B) log transformed frequency at Von Damm and Piccard.

Fig. S11. 16S archaeal (A) and bacterial (B) sequences identified from metagenomes for Ginger Castle (Von Damm) and Shrimp Gulley#2 (Piccard).

Fig. S12. Taxonomic annotation of key genes involved in hydrogen (green), methane (orange), nitrogen (purple), sulfur (blue), oxygen metabolism (grey) and in carbon fixation including Reductive TCA (red), Calvin Benson Bassham (yellow), 3-Hydroxpropionate/4-Hydroxybutyrate (cyan), and Reductive Acetyl-Coa (pink) at Von Damm and Piccard.

Fig. S13. COGs relative abundance of major categories of functional genes in the shotgun metagenomes obtained from Von Damm (inner circle) and Piccard (outer circle).

Fig. S14. Heat map showing the relative abundance of all KEGGs (Kyoto Encyclopedia of Genes and Genomes) in Von Damm and Piccard. The brightness (yellow) in the heat map reflects the abundance (copies per genome).

Fig. S15. Twenty most abundant functions in Von Damm versus Piccard (A) and Piccard versus Von Damm (B) annotated with KEGGS. The brightness (yellow) in the heat map reflects the abundance (copies per genome) of a particular function in a sample.

Table S1. Latitude, longitude and name of samples from this study.

Appendix S1. Methods.